

The $4^1\Sigma^+$ electronic state of LiCs molecule

Jacek Szczepkowski^{1,a}, Patryk Jasik², Anna Grochola³, Włodzimierz Jastrzębski¹, Józef E. Sienkiewicz², and Paweł Kowalczyk³

¹ Institute of Physics, Polish Academy of Sciences, al. Lotników 32/46, 02-668 Warszawa, Poland

² Department of Theoretical Physics and Quantum Information, Faculty of Applied Physics and Mathematics, Gdańsk University of Technology, ul. Narutowicza 11/12, 80-233 Gdańsk, Poland

³ Institute of Experimental Physics, Department of Physics, University of Warsaw, ul. Hoża 69, 00-681 Warszawa, Poland

Abstract. The $4^1\Sigma^+$ state of LiCs molecule is observed experimentally for the first time. The inverted perturbation approach (IPA) method is used to derive the potential energy curve of the state from the measured spectra. The experiment is accompanied by theoretical calculations of adiabatic potentials for excited states in LiCs including $4^1\Sigma^+$, performed with the MOLPRO program package. The irregular shape of the $4^1\Sigma^+$ state potential predicted by theory is confirmed in the experiment.

1 Introduction

Many excited states of diatomic molecules are associated with potential energy curves of shapes very different from the Morse potential. Such potentials, often referred to as 'exotic' ones, can be characterized by unusual bends, shelves or multiple minima, resulting from avoided crossings between the neighbouring states of the same symmetry [1]. Exotic molecular states are challenging for both theoreticians and experimentalists. Strong interaction between neighbouring electronic states must be handled with special care in calculations and the results provide exacting tests of their quality. On the other hand, band systems involving exotic states are marred by irregular spacing of spectral lines, making analysis of observed spectra a particularly demanding task.

The interest in electronic states with exotic potentials has been revived in recent years, especially in case of alkali metal dimers, by a progress in experiments on cold molecules. These states, which often exhibit unusually broad potential wells, may be employed as the final states of the photoassociation process. Additionally, they can be used as the intermediate states either for resonantly enhanced multiphoton ionization of photoassociated cold molecules or for their efficient transfer to the ground state [2].

In this paper we present first experimental study of the $4^1\Sigma^+$ state in LiCs molecule. The unusual shape of its potential curve results primarily from an anticrossing

with the lower $3^1\Sigma^+$ state. The state was observed through the $4^1\Sigma^+ \leftarrow X^1\Sigma^+$ transition recorded under rotational resolution. The experiment revealed that, because of unfavourable Franck-Condon factors, transitions to the lowest vibrational levels of the $4^1\Sigma^+$ state could not be observed in excitation from the thermally populated ground state levels. Moreover, the $4^1\Sigma^+$ state exhibits numerous local perturbations by neighbouring electronic states. Therefore interpretation of the observed spectra had to be aided by theoretical calculation of the manifold of electronic states situated in the investigated range of excitation energies. In the following sections we first describe computational details and results of calculations, then the measurements and data analysis leading to construction of the $4^1\Sigma^+$ state potential derived from experimental data and finally compare the experimental results with the theoretical predictions.

2 Theory

As the details of our theoretical approach have been already presented [3,4] only the salient information will be given here. Shortly, the calculations are based on the self consistent field configuration interaction (SCF CI) method with atomic effective core potentials and core polarization potentials, which enables to treat only two valence electrons explicitly. A reach basis of employed atomic orbitals allows us to obtain reliable results for adiabatic potentials of relatively high lying molecular states.

All calculations of the adiabatic potential energy curves are performed by means of the MOLPRO program package [5]. The core electrons of Cs atoms are represented by pseudopotential ECP54SDF [6]. We use the basis sets for cesium which comes with ECP54SDF [6] for s and p functions and ECP46MDF pseudopotential [7] for d and f functions. Additionally, these basis sets are augmented by thirteen s functions (10.635977¹, 6.149759, 3.555812, 2.055983, 1.445359, 1.188777, 0.687355, 0.132869, 0.070621, 0.009778, 0.005059, 0.002617, 0.001354), eight p functions (3.908238, 1.649125, 0.695867, 0.293629, 0.004186, 0.00183, 0.0008, 0.00035), eight d functions (44.566381, 16.875275, 6.389904, 2.419568, 0.007969, 0.003187, 0.001275, 0.00051) and four f functions (6.389902, 2.419568, 0.051637, 0.019922). In turn, for Li, the core electrons are represented by pseudopotential ECP2SDF [8]. This basis set is augmented by twelve s functions (1979.970927, 392.169555, 77.676373, 15.385230, 5.269282, 0.180366, 0.119550, 0.010159, 0.007920, 0.003894, 0.001493, 0.000572) and eleven p functions (470.456384, 96.625417, 19.845562, 4.076012, 0.567670, 0.141468, 0.035314, 0.007058, 0.002598, 0.000957, 0.000352). Additionally, for d and f functions we use cc-pv5z basis set [9] augmented by eight d functions (7.115763, 3.751948, 1.978300, 1.043103, 0.026579, 0.011580, 0.005046, 0.002199) and four f functions (0.885847, 0.556818, 0.055000, 0.027500).

We check the quality of our basis set performing the CI calculations for the ground and several excited states of isolated cesium and lithium atoms. The calculated adiabatic potentials correlate to the Cs($5d$) + Li($2s$), Cs($6s$) + Li($2p$) and Cs($7s$) + Li($2s$) atomic asymptotes. The potential energy curves for LiCs are computed using the complete active space self consistent field (CASSCF) method to generate the orbitals for the subsequent CI calculations. The corresponding active space in the $C_{\infty v}$ point group involves the molecular counterparts of the $6s$, $6p$, $5d$ and $7s$ valence orbitals of the Cs atom and $2s$, $2p$ valence orbitals of the Li atom.

The calculated potential energy curve of the $4^1\Sigma^+$ state is presented in Fig. 1. We also show the nearest states of the same symmetry, namely $3^1\Sigma^+$ and $5^1\Sigma^+$. We

¹ The numbers listed in parenthesis are the exponential coefficients of the Gaussian Type Orbitals (GTO).



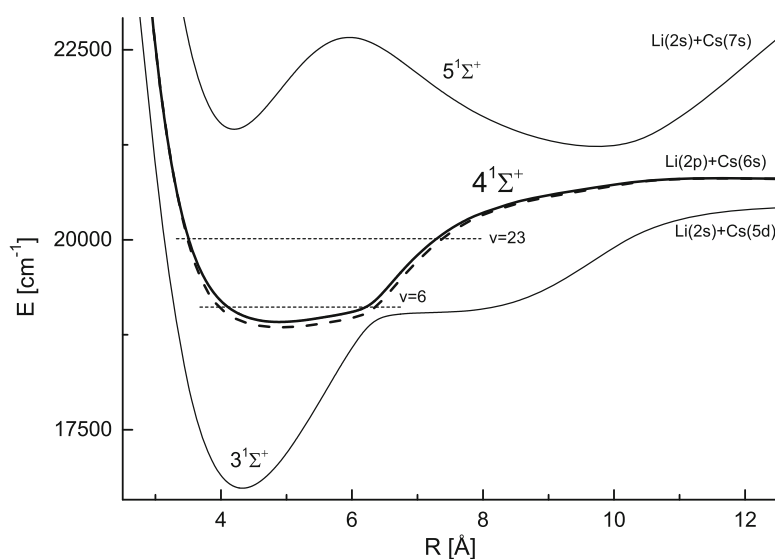


Fig. 1. Theoretical adiabatic potentials of the 3, 4 and $5^1\Sigma^+$ states in LiCs molecule (solid lines) compared with the experimental curve for $4^1\Sigma^+$ (dashed line). The range of observed vibrational levels is shown and the corresponding atomic asymptotes indicated.

Table 1. Main molecular constants for the $4^1\Sigma^+$ excited state of the LiCs molecule.

| Author | R_e [Å] | D_e [cm^{-1}] | ω_e [cm^{-1}] | T_e [cm^{-1}] |
|-----------------------------|-----------|----------------------------|---------------------------------|----------------------------|
| Present work exp. | 4.91 | 1931 | 39.7 | 18848.4 |
| Present work theory | 4.885 | 1863 | 44.76 | 18918 |
| Dardouri et al. theory [17] | 5.00 | 1610 | | 19081 |
| Mabrouk et al. theory [18] | 5.01 | 1856 | 44.57 | 19081 |
| Korek et al. theory [19] | 4.98 | 1908 | 45.74 | 18998 |

notice avoided crossing between the potential curves of the $4^1\Sigma^+$ and $5^1\Sigma^+$ states at around 10 Å. The second, very characteristic avoided crossing between the $3^1\Sigma^+$ and $4^1\Sigma^+$ states is visible at around 6.4 Å. It is also worth to mention that the $4^1\Sigma^+$ potential energy curve has a small barrier with maximum at around 11.6 Å lying 30 cm^{-1} above the atomic asymptote. The reason for its formation is the proximity of the atomic asymptotes $\text{Li}(2s) + \text{Cs}(5d)$ and $\text{Li}(2p) + \text{Cs}(6s)$. Due to the above facts the shape of the investigated state is very irregular. In Table 1 we compare molecular constants derived from the calculated $4^1\Sigma^+$ state potential with results of previous theoretical works and values obtained in the experimental part of this study.

3 Experiment

The experimental arrangement used by us has been described elsewhere [10,11] and therefore it will be not presented here. In brief, we employ a V-type optical-optical double resonance polarization labelling spectroscopy method with two independent pump and probe lasers. The molecular source is a dual temperature heat pipe oven [12] containing LiCs vapour. The apparatus provides us with rotationally resolved molecular spectra with both resolution and accuracy slightly better than 0.1 cm^{-1} . In the investigated spectral range $18150 - 20100 \text{ cm}^{-1}$ we observed around 400 spectral lines assigned to the $4^1\Sigma^+ \leftarrow X^1\Sigma^+$ band system. The measured line positions

were subsequently transformed to energies of rovibrational levels in the upper state employing the precisely known ground state level energies [13]. These data were used then to construct the experimental potential energy curve of the $4^1\Sigma^+$ state. Because the molecular potential was expected to be of an exotic form, hard to represent by any analytical formula, we have chosen a numerical representation by a set of grid points $\{R_k, U_k\}$ interpolated with cubic spline functions. The initial, 'guessed' potential curve was optimized iteratively with the inverted perturbation approach (IPA) method [14], by minimizing differences between the calculated eigenenergies and their experimentally determined counterparts. It is always advisable to choose a reasonable initial potential energy curve for the IPA procedure, as it affects stability and rate of convergence of the routine, and the theoretical curve described in the previous section was the obvious choice. However, the main problem in the analysis was that in our experiment the lowest vibrational levels of the $4^1\Sigma^+$ state were inaccessible from the levels labelled in the ground state (because of insufficient Franck-Condon overlap). Therefore we could not establish vibrational numbering in the $4^1\Sigma^+$ state directly. On the other hand, we also could not rely on the numbering suggested by the theoretical potential, because it is known that theoretical curves usually depict better the actual shape of the potential than its position in the energy scale. Therefore we repeated the IPA optimization assuming several initial potentials, each of the shape of the theoretical one but shifted in energy and thus imposing different vibrational numbering on the observed levels. As a result of many runs of the IPA routine, several improved potential curves have been generated, each of them reproducing equally well the experimental levels. Then for every curve the Franck-Condon intensities were calculated for the $4^1\Sigma^+ \leftarrow X^1\Sigma^+$ band system and compared with the intensity patterns in the vibrational progressions observed experimentally. It turned out that only one of the potentials reproduces correctly characteristic positions of intensity minima in the observed spectra and the corresponding vibrational numbering should be considered the correct one, although a change by plus or minus one vibrational number is not fully excluded.

Another problem encountered during the analysis consists in numerous strong, local perturbations of the $4^1\Sigma^+$ state which at their peaks may cause shift of rovibrational levels up to 9 cm^{-1} . As the abundance of perturbations did not allow us to select the unperturbed levels undoubtedly, we included all of them into the fit but in each iteration controlled smooth shape of the molecular potential with regularization procedure [15]. Additionally, to decrease the influence of perturbed levels on the fit we applied the robust fitting method proposed by Watson [16], in which the statistical weights of levels that systematically deviate from the expected positions are diminished according to their residuals.

The final potential energy curve of the $4^1\Sigma^+$ state (see Fig. 1) is given in a grid of 80 points. The energy levels used in the analysis correspond to $v' = 6 - 23$ enabling definition of the experimental potential between 3.4 and 7.5 Å. Because of perturbations of the state, the observed rovibrational levels are reproduced by the potential with a standard deviation of 3.5 cm^{-1} . Although some spectroscopic applications require higher accuracy, it is more than sufficient for testing of theoretical calculations.

4 Concluding remarks

The detailed numerical data related to the experimental and theoretical work are deposited at the web pages <https://dimer.ifpan.edu.pl> and http://aqualung.mif.pg.gda.pl/lics_4ssigma. A comparison of both potential curves for the $4^1\Sigma^+$ state reveals that the calculations reproduce the experimental



shape of the molecular potential very well, except of the potential depth, too small by about 70 cm^{-1} . This shows a remarkable progress in modern quantum chemistry calculations, now capable of predicting correct shapes even for exotic molecular potentials displaying prominent anticrossings.

The Warsaw team acknowledges partial funding by the KBN grant No. N202 203938. The Gdansk group acknowledges partial support by the COST action CM0702 of the European Community and the Polish Ministry of Science and Higher Education under grant No. 645/N – COST/2010/0.

References

1. J. von Neumann, E. Wigner, *Phys. Z.* **30**, 467 (1929)
2. K.M. Jones, E. Tiesinga, P.D. Lett, P.S. Julienne, *Rev. Mod. Phys.* **78**, 483 (2006)
3. P. Jasik, J.E. Sienkiewicz, *Chem. Phys.* **323**, 563 (2006)
4. P. Łobacz, P. Jasik, J.E. Sienkiewicz, *Cent. Eur. J. Phys.* (in print) doi: 10.2478/s11534-012-0137-5
5. MOLPRO, version 2006.1, a package of ab initio programs, H.-J. Werner, P.J. Knowles, et al., see [<http://www.molpro.net>]
6. L. Von Szentpaly, P. Fuentealba, H. Preuss, H. Stoll, *Chem. Phys. Lett.* **93**, 555 (1982)
7. I.S. Lim, P. Schwerdtfeger, B. Metz, H. Stoll, *J. Chem. Phys.* **122**, 104103 (2005)
8. P. Fuentealba, H. Preuss, H. Stoll, L. Von Szentpaly, *Chem. Phys. Lett.* **89**, 418 (1982)
9. D. Feller (unpublished)
10. W. Jastrzębski, P. Kowalczyk, *Phys. Rev. A* **51**, 1046 (1995)
11. J. Szczepkowski, A. Grochola, W. Jastrzębski, P. Kowalczyk, *J. Mol. Spectrosc.* **276-277**, 19 (2012)
12. A. Grochola, J. Szczepkowski, W. Jastrzębski, P. Kowalczyk, *J. Chem. Phys.* **135**, 044318 (2011)
13. P. Staunum, A. Pashov, H. Knöckel, E. Tiemann, *Phys. Rev. A* **75**, 042513 (2007)
14. A. Pashov, W. Jastrzębski, P. Kowalczyk, *Comput. Phys. Commun.* **128**, 622 (2000)
15. A. Grochola, P. Kowalczyk, W. Jastrzębski, A. Pashov, *J. Chem. Phys.* **121**, 5754 (2004)
16. J.K.G. Watson, *J. Mol. Spectrosc.* **219**, 326 (2003)
17. R. Dardouri, K. Issa, B. Oujia, F.X. Gadéa, *Int. J. Quantum Chem.* **112**, 2724 (2012)
18. N. Mabrouk, H. Berriche, H. Ben Ouada, F.X. Gadea, *J. Phys. Chem. A* **114**, 6657 (2010)
19. M. Korek, A.R. Allouche, K. Fakhreddine, A. Chalan, *Can. J. Phys.* **78**, 977 (2000)